# Direct writing of liquid metal microheaters for microvalve applications

Navid Hussain*, Alexander Scholz*, Tobias Spratte†, Christine Selhuber-Unkel†, Michael Hirtz* and Jasmin Aghassi-Hagmann*

*Institute of Nanotechnology (INT), Karlsruhe Institute of Technology (KIT), Hermann-von-Helmholtz-Platz 1, 76344 Eggenstein-Leopoldshafen, Germany.

†Institute for Molecular Systems Engineering and Advanced Materials (IMSEAM), INF 225, Heidelberg University, 69120 Heidelberg, Germany.

***Abstract*— This paper presents the direct writing of liquid metal (LM) based microheaters for microvalve applications based on thermo-responsive polymers. In LM microheaters, rising temperatures (usually beyond 50 °C) can lead to voids formation or electromigration, resulting in failure. To prevent this, multiple layers of liquid metal lines can be printed, increasing their overall height. Experimentally, this method results in more stable and durable microheaters compared to thin, one-time printed wires. These microheaters can withstand temperatures above 160 °C without breakage.**

***Keywords—Galinstan, microheaters, printed electronics.***

## I. INTRODUCTION

The rapid growth of flexible and printed electronics has prompted researchers to turn their attention to liquid metals (LMs), which exhibit the same electrical and thermal conductivity as many conventional metals and alloys [1], [2]. In addition, LMs are both ductile and fluid at or near room temperature (RT), enabling printing and direct writing without the need for subsequent annealing processes [3].

Direct patterning of the gallium-based LM alloys provides diverse applications of LMs such as flexible sensors [4]–[7], self-healing interconnects wires and sensors [8], [9], stretchable interconnects, wires and electronic components [10], [11], printed diodes and transistors [3], [12], flexible display devices [13], wearable electronics and biological prosthetic devices [14], [15], and implantable and epidermal electronics [16]. Recently, also LM-based microheaters have been reported [17], [18]. However, these microheater structures were fabricated with microchannel-based systems, which can be complex in design, include multiple fabrication steps, and are not flexible in layout. Moreover, these microheaters based on liquid metal are susceptible to the breakage caused by voids forming in the liquid metal as temperatures rise above ~100 °C [17]. To remove the multiple steps involved and simplify the microheater fabrication, direct writing of LM-based microheaters is an attractive option. Furthermore, the problem with breakage of LM microheater structures at high temperatures can be resolved when applying direct writing of LM microheaters.

In this work, we present experimental results from direct written LM microheaters. Additionally, we demonstrate a microvalve application based on the devices developed.

## II. EXPERIMENTAL

First, macroscopic electrodes were manually deposited by hand on the freshly cleaned glass substrate for a contact using Ag epoxy paste (Elecolit® 3653 10g). Galinstan (LM) [19] microheater line structures were printed using the previously reported [3] glass capillary-based direct writing method.

All printed microheater structures were investigated with a Nikon Eclipse 80i upright optical microscope. The minimum line width of the LM-based microheater structures is around 20 µm (Figure 1b), and the average line width of the LM lines for microheaters investigated in the experiments is about 100 µm, if not otherwise mentioned. A Keithley 2000 multimeter was used to test the resistance of the devices. A Keysight B2902A source measure unit (SMU) was used to apply a voltage across the heater. Microheater structures were kept uncoated during all the experiments. The experiments were performed at room temperature and under ambient conditions.

The temperature distributions of the microheater were measured by an advanced thermography system, Bosch professional GTC 400C, which has a visual camera integrated with an infrared sensor achieving a resolution of 160 x 120 pixels for the thermal image. The camera was placed near the microheater surface to provide detailed thermal images.

## III. RESULTS

### A. Analysis of LM microheaters

In order to acquire resistance vs. temperature data, each microheater was heated on a hotplate at different temperatures. When the microheater temperature was maintained at higher temperatures (around more than 60 °C) for a longer duration, the resistance of the printed structures kept on increasing even after approximately 5 minutes, so for consistency the resistance values were acquired after 15min of temperature settling time for each data point. The measured electrical resistance of the microheaters with respect to temperature was in accordance to similar previous reports [20].

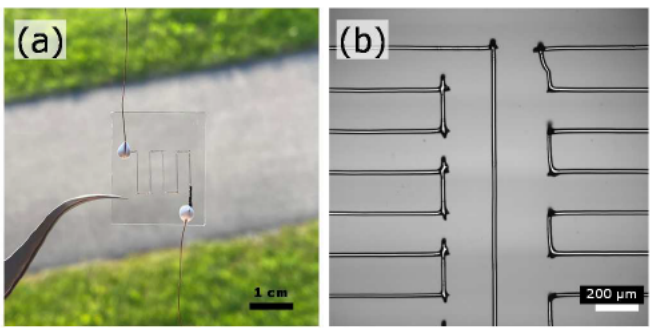


Fig. 1. (a) Photo of LM microheaters. (b) Optical microscope images of microheater structures on glass.

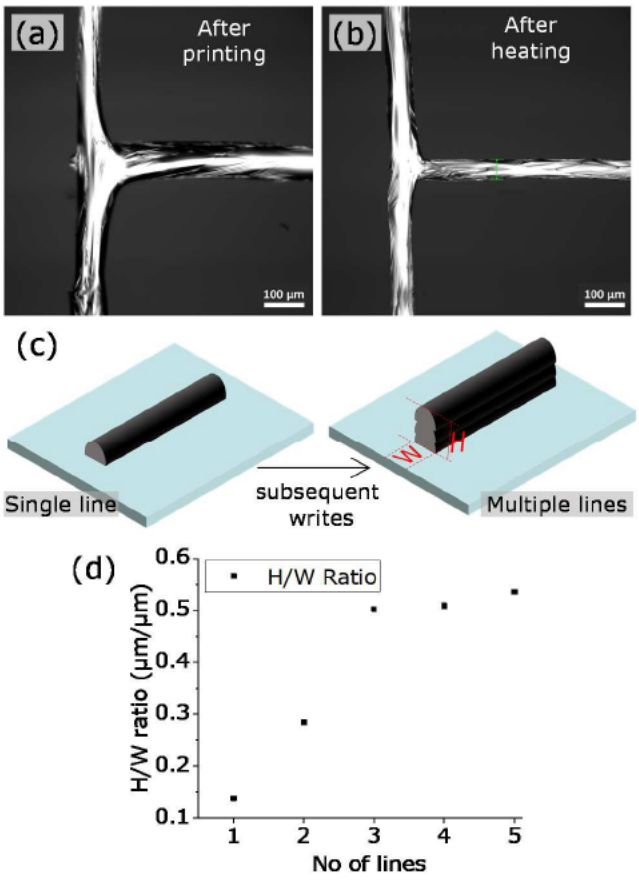


Fig. 2. Optical microscope images of a LM microheater structure (a) after printing and (b) after heating. (c) Printing multiple layers on top of each other increases the pattern's height and provides more temperature-stable structures. (d) Aspect ratio of height (calculated with Z-series imaging in NIS elements imaging software) and width of printed Galinstan lines. The width and height are also subject to distance between tip and substrate.

When applying a voltage over the device, it was observed that at temperatures beyond approximately 50 °C, some LM lines started to degenerate, which was visible in a massive increase of resistance until the connection failed completely.

When observed under the microscope (Figure 2), these LM structures show shrinkage (Figure 2b) in the width of the LM line. It might be that LM displaces or voids are formed underneath the oxide layer as, during heating, a thermal gradient is formed. This is a known challenge for LM-based devices that are subjected to high temperatures, causing them to break [17], [18]. There have been two hypotheses proposed to explain why voids can form in LM structures, which are either attributed to metallic electromigration effects [18] or a mismatch between temperature expansion coefficients (TEC) (in the case of LM filled in PDMS microchannels) [17].

In our case, the shrinking of the LM line, as shown in Figures 2a,b, and the breaking of LM lines can be explained by electromigration theory [21], [22]. For microfluidic-based devices, a proposed solution to avoid the voids is to continuously inject LM into the microfluidic channels [17]. However, this only partially solves the problem and generates new issues. Despite its effectiveness in filling voids and generating a uniform temperature field, this approach needs an additional pump to supply LM, and raises material consumption [17]. However, for direct written LM microheaters, the problem of failing connections can be alleviated by printing multiple layers on top of each other (Figure 2c) and thus increasing the height (Figure 2d) of the pattern. This approach enables the fabrication of more stable microheater structures, which were then further characterized.

### *B. Thermal parameter characterization*

Several thermal parameters should be considered when choosing a microheater, including its power consumption and response time [23], [24]. Two samples (P-T_sample1 and 2) were printed via the LM direct writing method, resulting in an

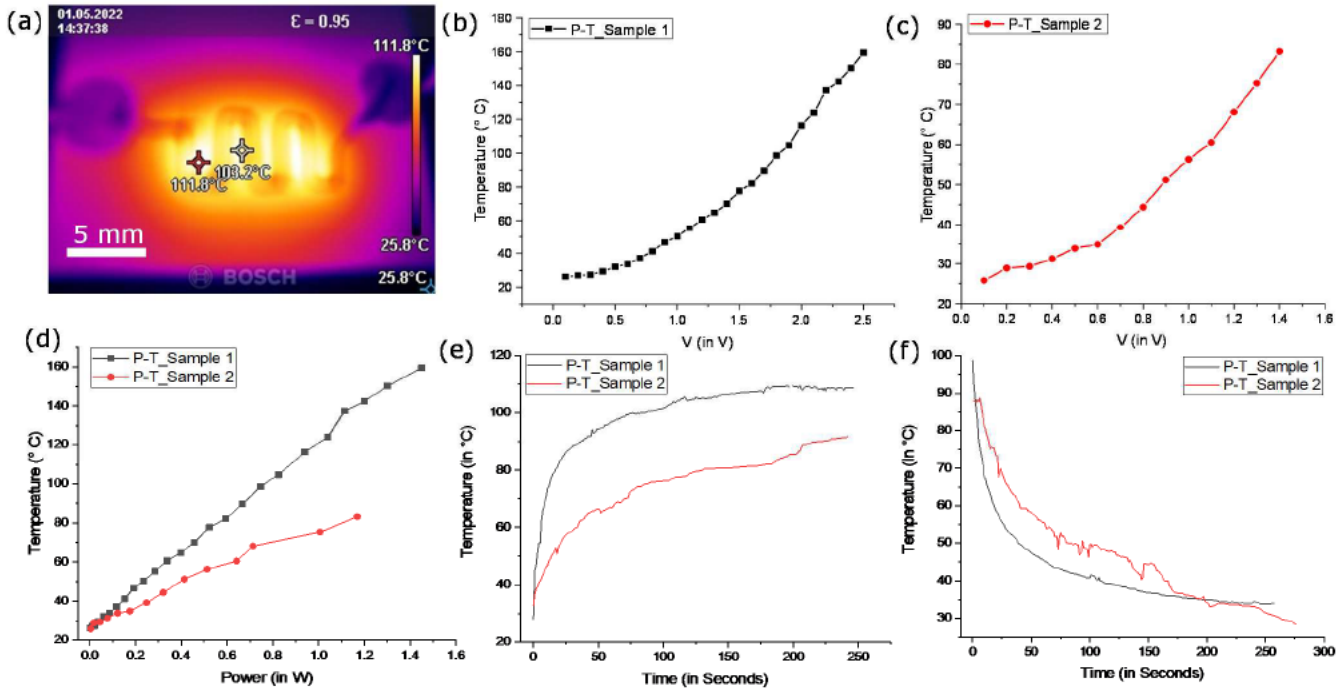


Fig. 3. (a) A thermogram showing the temperature distribution for a typical microheater structure. Recorded maximum surface temperature with respect to the (b), (c) voltage, and (d) power applied. The heating (e) and cooling (f) response times for both LM microheaters where a voltage of 1.5V and 2 V are applied, resulting in a 0.92 W and 1.54 W power consumption in LM microheaters P-T_Sample 1 and 2, respectively.

average line width of 108.49 ± 4.54 µm. The samples were fabricated by printing multiple lines, each of 1 cm in length: 8 lines and 5 lines, at a pitch of 1000 µm and 3000 µm, and connected to form meander shapes, finally providing a total length of meander LM structures around 9.3 cm and 6.9 cm for P-T_sample1 and 2 respectively, connected to the macroscopic Ag electrodes. The process was repeated 5 times and 3 times with moving 10 µm away from the substrate in each layer, providing height of 54.81 and 68.44 µm (calculated with Z-series imaging in NIS elements imaging software) for P-T_sample1 and 2 respectively. The resistance of each sample was monitored before and after the heating and temperature measurement; it remained at 3.5 Ω and 1.4 Ω for P-T_sample1 and 2, respectively.

Then, the structures were characterized for power consumption and achievable temperature response. The microheaters were subjected to DC voltages between 0.1 and 2 V, and voltage was increased by 0.1 V, and maximum local temperatures at the substrate's center were measured. To achieve thermal equilibrium, the time interval between each applied input voltage was set to 15 minutes. Figure 3 shows the thermal response curve of the LM microheaters, which reveals the maximum achieved microheater temperature of 159.4 and 83.2 °C for P-T_Sample 1 and 2, respectively.

In order to determine the heating response time, the microheater was turned instantly onto the power of 0.92W and 1.54 W for P-T_Sample 1 and 2, respectively. After reaching a steady state, the power was turned off, and the time it took to reach room temperature was recorded to investigate the cooling response time. While heating (Figure 3e), microheater P-T_Sample 1 reaches a steady state in around 175 s, and P-T_Sample 2 reaches a plateau after around 250 s. While cooling (Figure 3f), both samples take around 250 s to reach near room temperature again.

### C. *Microvalve application*

As an example of a direct write microheater application, we demonstrate a microvalve for fluid flow control. For this purpose, a thermoresponsive poly(*N*-isopropylacrylamide) (PNIPAM) based hydrogel was used, which is a stimuli-responsive material that shows mechanical response as well as volume change when heated [25]. Hydrogels based on PNIPAM can be easily prepared in water [26]. A PNIPAM solution undergoes a reversible lower critical solution temperature (LCST) phase transition from its soluble hydrated state to its insoluble dehydrated state at temperatures higher than their cloud point. Typically, this transition occurs at 32 °C [27], [28]. For the demonstration as a microvalve, a commercially available microchannel (from ibidi) was functionalized with the PNIPAM and a microheater, and used to gate a fluorescent liquid (perovskite quantum dot solution (QDs)) and ethanol for visualization purposes. PNIPAM was manually deposited by hand in a microchannel, and a microscope glass slide was attached to the microchannel side, then the PNIPAM valve was cured with UV light. The microchannel was filled with perovskite quantum dots solution on one side and ethanol on the other. A microheater structure was then installed on the ibidi chip.

The microvalve and microchannel is observed under a fluorescence microscope (Figure 4) to monitor its gating activity. Applying voltage to the microheater causes the PNIPAM barrier to shrink, allowing the mixing of fluorescent perovskite QD solution with non-fluorescent ethanol, which is

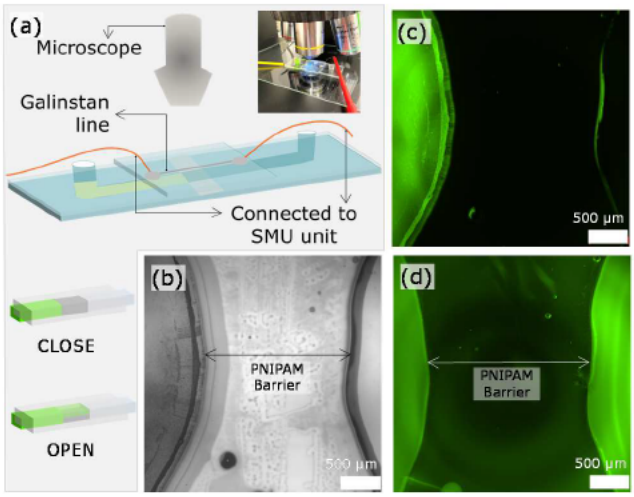


Fig. 4. Microheater for microvalve application. (a) Schematics of the complete setup and actual photograph of the setup (inset). Microscope images of the PNIPAM barrier and adjacent QD liquid (b) in bright field and (c) in fluorescence with FITC filter (B-2E/C, Nikon, Ex.: 465–495 nm, Em.: 515–555 nm). (d) shows a fluorescent image of the microchannel after triggering the PNIPAM valve by heating, allowing the fluorescent QDs to diffuse into the other parts of the channel structures.

monitored using bright field and fluorescence images (Figure 4b-c). After around eight minutes (showing that the barrier is effective in blocking the QDs), the gate is opened and the fluorescent QDs diffuse into the right part of the channel (Figure 4d).

This simple demonstrator shows the feasibility of microheater/PNIPAM valve devices for liquid gating. In the future, these LM structures could also be modified to regulate the flow between two fluidic ports and more complicated microfluidic networks.

## IV. Conclusion

In this paper, we present the direct writing of LM-based microheaters with meander structure design on glass substrates. In the fabricated microheaters, optical microscopy reveals an average LM line width of around ~100 µm, with a minimum line width of around 20 µm. The LM microheater structures were characterized for the voltage applied, power consumption, and heating and cooling response time. The investigated LM microheater structures can reach a temperature of 160 °C. The maximum voltage applied is 2.5 V, and the power consumption is 0.92 W. These structures also have an extremely fast response time, able to reach beyond 100 °C in 150 seconds, which is much shorter than previously observed microchannel-based LM microheaters. The main advantage of direct writing of LM microheaters is that it offers – as a digital and additive process - freedom of design as no mask or microchannel mold is needed. Also, in comparison to other microheaters based on Pt, Au, or Ag, these LM microheaters are more cost-effective.

## Acknowledgment

This work was carried out with the support of the Karlsruhe Nano Micro Facility (KNMFi, www.knmf kit.edu), a Helmholtz Research Infrastructure at Karlsruhe Institute of Technology (KIT, www.kit.edu). The work was supported by Deutsche Forschungsgemeinschaft (DFG) under 3D Matter Made to Order (3DMM2O) – Cluster of Excellence, by the SPP 2206 KOMMMA (SE 1801/4-1). A.S. acknowledges financial support from the BMBF project SensIC.

## REFERENCES


[1] T. Liu, P. Sen, and C. J. Kim, "Characterization of nontoxic liquid-metal alloy galinstan for applications in microdevices," *Journal of Microelectromechanical Systems*, vol. 21, no. 2, pp. 443–450, Apr. 2012.

[2] M. D. Dickey, R. C. Chiechi, R. J. Larsen, E. A. Weiss, D. A. Weitz, and G. M. Whitesides, "Eutectic Gallium-Indium (EGaIn): A Liquid Metal Alloy for the Formation of Stable Structures in Microchannels at Room Temperature," *Adv Funct Mater*, vol. 18, no. 7, pp. 1097–1104, Apr. 2008.

[3] N. Hussain *et al.*, "High-Resolution Capillary Printing of Eutectic Gallium Alloys for Printed Electronics," *Adv Mater Technol*, vol. 6, no. 11, p. 2100650, Nov. 2021.

[4] J. W. Boley, E. L. White, G. T. C. Chiu, and R. K. Kramer, "Direct Writing of Gallium-Indium Alloy for Stretchable Electronics," *Adv Funct Mater*, vol. 24, no. 23, pp. 3501–3507, Jun. 2014.

[5] S. Ali *et al.*, "Flexible Capacitive Pressure Sensor Based on PDMS Substrate and Ga-In Liquid Metal," *IEEE Sens J*, vol. 19, no. 1, pp. 97–104, Jan. 2019.

[6] K. Bugra Ozutemiz *et al.*, "EGaIn–Metal Interfacing for Liquid Metal Circuitry and Microelectronics Integration," *Adv Mater Interfaces*, vol. 5, no. 10, p. 1701596, May 2018.

[7] C. B. Cooper *et al.*, "Stretchable Capacitive Sensors of Torsion, Strain, and Touch Using Double Helix Liquid Metal Fibers," *Adv Funct Mater*, vol. 27, no. 20, p. 1605630, May 2017.

[8] G. Li, X. Wu, and D. W. Lee, "Selectively plated stretchable liquid metal wires for transparent electronics," *Sens Actuators B Chem*, vol. 221, pp. 1114–1119, Dec. 2015.

[9] M. D. Dickey, "Stretchable and Soft Electronics using Liquid Metals," *Advanced Materials*, vol. 29, no. 27, p. 1606425, Jul. 2017.

[10] C. Ladd *et al.*, "3D Printing of Free Standing Liquid Metal Microstructures," *Advanced Materials*, vol. 25, no. 36, pp. 5081–5085, Sep. 2013.

[11] H. Zhu, S. Wang, M. Zhang, T. Li, G. Hu, and D. Kong, "Fully solution processed liquid metal features as highly conductive and ultrastretchable conductors," *npj Flexible Electronics 2021 5 1*, vol. 5, no. 1, pp. 1–8, Sep. 2021.

[12] R. C. Ordonez *et al.*, "Rapid Fabrication of Graphene Field-Effect Transistors with Liquid-metal Interconnects and Electrolytic Gate Dielectric Made of Honey," *Scientific Reports 2017 7 1*, vol. 7, no. 1, pp. 1–9, Aug. 2017.

[13] M. Wang, X. Feng, X. Wang, S. Hu, C. Zhang, and H. Qi, "Facile gelation of a fully polymeric conductive hydrogel activated by liquid metal nanoparticles," *J Mater Chem A Mater*, vol. 9, no. 43, pp. 24539–24547, Nov. 2021.

[14] Y. Ren, X. Sun, and J. Liu, "Advances in Liquid Metal-Enabled Flexible and Wearable Sensors," *Micromachines 2020, Vol. 11, Page 200*, vol. 11, no. 2, p. 200, Feb. 2020.

[15] Y. G. Park, G. Y. Lee, J. Jang, S. M. Yun, E. Kim, and J. U. Park, "Liquid Metal-Based Soft Electronics for Wearable Healthcare," *Adv Healthc Mater*, vol. 10, no. 17, p. 2002280, Sep. 2021.

[16] X. Wang, Y. Zhang, R. Guo, H. Wang, B. Yuan, and J. Liu, "Conformable liquid metal printed epidermal electronics for smart physiological monitoring and simulation treatment," *Journal of Micromechanics and Microengineering*, vol. 28, no. 3, p. 034003, Feb. 2018.

[17] J. Je and J. Lee, "Design, fabrication, and characterization of liquid metal microheaters," *Journal of Microelectromechanical Systems*, vol. 23, no. 5, pp. 1156–1163, Oct. 2014.

[18] L. Zhang *et al.*, "A Performance-Enhanced Liquid Metal-Based Microheater with Parallel Ventilating Side-Channels," *Micromachines 2020, Vol. 11, Page 133*, vol. 11, no. 2, p. 133, Jan. 2020.

[19] T. Liu, P. Sen, and C. J. Kim, "Characterization of liquid-metal Galinstan® for droplet applications," *Proceedings of the IEEE International Conference on Micro Electro Mechanical Systems (MEMS)*, pp. 560–563, 2010.

[20] Y. Plevachuk, V. Sklyarchuk, S. Eckert, G. Gerbeth, and R. Novakovic, "Thermophysical properties of the liquid Ga-In-Sn eutectic alloy," *J Chem Eng Data*, vol. 59, no. 3, pp. 757–763, Mar. 2014.

[21] R. Ma, C. Guo, Y. Zhou, and J. Liu, "Electromigration Induced Break-up Phenomena in Liquid Metal Printed Thin Films," *Journal of Electronic Materials 2014 43 11*, vol. 43, no. 11, pp. 4255–4261, Aug. 2014.

[22] H. O. Michaud and S. P. Lacour, "Liquid electromigration in gallium-based biphasic thin films," *APL Mater*, vol. 7, no. 3, p. 031504, Feb. 2019.

[23] Z. E. Jeroish, K. S. Bhuvaneshwari, F. Samsuri, and V. Narayanamurthy, "Microheater: material, design, fabrication, temperature control, and applications—a role in COVID-19," *Biomed Microdevices*, vol. 24, no. 1, pp. 1–49, Mar. 2022.

[24] P. Bhattacharyya, "Technological journey towards reliable microheater development for MEMS gas sensors: a review," *IEEE Transactions on Device and Materials Reliability*, vol. 14, no. 2, pp. 589–599, 2014.

[25] M. A. Haq, Y. Su, and D. Wang, "Mechanical properties of PNIPAM based hydrogels: A review," *Materials Science and Engineering C*, vol. 70, pp. 842–855, Jan. 2017.

[26] H. Tokuyama, N. Ishihara, and S. Sakohara, "Effects of synthesis-solvent on swelling and elastic properties of poly(N-isopropylacrylamide) hydrogels," *Eur Polym J*, vol. 43, no. 12, pp. 4975–4982, Dec. 2007.

[27] A. Halperin, M. Kröger, and F. M. Winnik, "Poly(N-isopropylacrylamide) Phase Diagrams: Fifty Years of Research," *Angewandte Chemie International Edition*, vol. 54, no. 51, pp. 15342–15367, Dec. 2015.

[28] M. Heskins and J. E. Guillet, "Solution Properties of Poly(N-isopropylacrylamide)," *Journal of Macromolecular Science Part A - Chemistry*, vol. 2, no. 8, pp. 1441–1455, Dec. 2006.